J Mater Sci (2009) 44:3900–3904
DOI 10.1007/s10853-009-3507-7

LETTER

Bridging stresses from R-curves of silicon nitrides

S. Fünfschilling · T. Fett · M. J. Hoffmann · R. Oberacker · H. Jelitto · G. A. Schneider · M. Härtelt · H. Riesch-Oppermann

Received: 10 February 2009 / Accepted: 18 April 2009 / Published online: 13 May 2009

The increasing crack resistance (R-curve) behaviour of ceramic materials is of high interest for technical applications. The initial value at the onset of crack extension is called the crack-tip toughness K_{I0}. Very often but not in all cases a saturation of $K_R \rightarrow K_{R,max}$ is observed. Whereas silicon nitride ceramics show an increase of K_R up to saturation within a few micrometers, alumina exhibits a comparably low initial steepness and shows saturation even after some mm crack extension.

Several reasons can be responsible for this effect. In coarse-grained materials, large grains can transmit tractions between the two crack faces resulting in so-called bridging stresses acting against the crack opening. As the consequence, such bridging effects shield the crack tip partially from the applied loads.

R-curve behaviour is commonly described by a relation $K_R = f(\Delta a)$ in which K_R is the stress intensity factor necessary for crack propagation by an amount of Δa. This would be an appropriate description for the case that the R-curves were pure material properties. In the past it has been shown by experimental and theoretical investigations that the R-curve is not a unique material property [1].

S. Fünfschilling (✉) · T. Fett · M. J. Hoffmann · R. Oberacker
Institut für Keramik im Maschinenbau, Universität Karlsruhe, Karlsruhe, Germany
e-mail: fuenfschilling@ikm.uni-karlsruhe.de

H. Jelitto · G. A. Schneider
Institut für keramische Hochleistungswerkstoffe, Technische Universität Hamburg-Harburg, Hamburg, Germany

M. Härtelt · H. Riesch-Oppermann
Institut für Materialforschung II, Forschungszentrum Karlsruhe, Karlsruhe, Germany

It is the common opinion that in the special case of R-curves caused by grain bridging effects, the relation between the bridging stresses, σ_{br}, and crack opening displacement, δ, $\sigma_{br} = f(\delta)$, is the intrinsic material property which is expected to be much less influenced by test conditions as geometry of the test specimen or special type of loading (tension, bending, etc.) [2].

For high-strength applications, silicon nitride (SN) ceramics are of high importance. Consequently, many R-curve measurements on this material class were carried out in literature and different methods were applied to determine the bridging law [3].

Direct measurements of the loads transferred by the bridges were performed by Pezzotti et al. [4, 5] and Kruzic et al. [6] applying Raman spectroscopy. A very popular method to determine the bridging stress relation is the evaluation of crack opening displacement (COD) measurements. This method was used by Fett et al. [7].

A procedure that allows the bridging stresses to be determined from existing R-curve results was developed in [8] and applied to coarse-grained alumina. This procedure should be used for R-curve measurements on silicon nitrides obtained by a high-resolution compliance method [9] to evaluate the bridging stresses.

The procedure of the determination of the bridging stresses is shown on two silicon nitride ceramics. Material (Y_2O_3, MgO)- SN is a silicon nitride which was consolidated in a two step sintering process. The powder mixture of Silicon nitride, 5 wt% Y_2O_3, and 2 wt% MgO was prepared by attrition milling in isopropanol and afterwards dried and sieved. Greenbodies ($45 \times 64 \times 6$ mm^3) were uniaxially pressed and subsequently cold- isostatically densified. The samples were sintered in a hot- isostatic-press. In the first step with a low N_2 pressure of 1 MPa, the samples were sintered to achieve closed porosity at a temperature of 1750 °C. Full density was achieved in the HIP step at an N_2 pressure of 20 MPa and a temperature of 1800 °C. Material (Y_2O_3, Al_2O_3) – SN is a commercial silicon nitride containing Y_2O_3 and Al_2O_3 (SL200BG, CeramTec, Plochingen, Germany).

R-curves for the two silicon nitride ceramics are represented in Fig. 1. The intrinsic toughness for the (Y_2O_3, MgO) is $K_{I0} = 2.33\ \text{MPa}\sqrt{\text{m}}$ [10] and for the commercial silicon nitride (Y_2O_3, Al_2O_3) $K_{I0} = 2.0\ \text{MPa}\sqrt{\text{m}}$. Figure 2b shows very steep R-curves at small crack extensions in both cases.

The R- curves can be described by

$$K_R = K_{I0} - K_{sh}\ , \quad K_{sh} < 0 \tag{1}$$

with the shielding stress intensity factor, K_{sh}, which causes through the crack tip shielding the R- curve behaviour. This fact allows the shielding stresses to be determined. The necessary procedures are extensively outlined in literature. For our purpose we used the technique described in [8].

For silicon nitride ceramics, the shielding effect is caused by bridging interactions in the crack wake by, e.g. grain bridging or grain pull- out, i.e.

$$K_{sh} = K_{br} \tag{2}$$

The bridging stresses σ_{br} acting against crack opening depend on opening displacements δ. Using the weight function representation, the bridging stress intensity factor is given by

$$K_{br} = \int_0^a h(x,a)\,\sigma_{br}[\delta(x)]\,dx \tag{3}$$

with the fracture mechanics weight function h for a crack ahead of a sharp notch (for details see [11]). The bridging displacements $\delta_{br} < 0$ are

$$\delta_{br} = \frac{1}{E'}\int_x^a h(x,a')da' \int_0^{a'} h(x'a')\,\sigma_{br}(x')dx' = \delta - \delta_{appl} \tag{4}$$

In (4), δ_{appl} is the displacement that would occur for an applied stress intensity factor K_{appl} in the absence of bridging stresses. These displacements are given by

$$\delta_{appl} = \frac{1}{E'}\int_x^a h(x,a')K_{appl}(a')da' \tag{4a}$$

with the stress intensity factor K_{appl} caused by the externally applied load. The system of Eqs. 3 and 4 can be solved by successive approximation or other numerical strategies. Here the simplest approach may be addressed.

For this purpose the bridging law $\sigma_{br} = f(\delta)$ may be expressed by a series expansion with respect to δ with unknown coefficients A_n

$$\sigma_{br} = \sum_{n=0}^{\infty} A_n\delta^n \cong \sum_{n=0}^{N} A_n\delta^n \tag{5}$$

For practicability, the infinite upper series limit may be replaced by a finite number of $N \gg 1$.

In the first step, the crack opening displacement field for an arbitrarily chosen crack length, a, is approximated by $\delta = \delta_{appl}$. This yields from (5) the bridging stress distribution $\sigma_{br}(x) = f(\delta_{appl}(x))$ for an arbitrarily chosen set of coefficients A_n. By using this distribution as the integrand of (4), a first approximation of bridging displacements and, consequently, an improved solution for the total displacements is obtained. In the next step, these improved δ-values are entered in (5) providing an improved bridging stress, etc. The procedure is repeated until a certain state of convergence is reached.

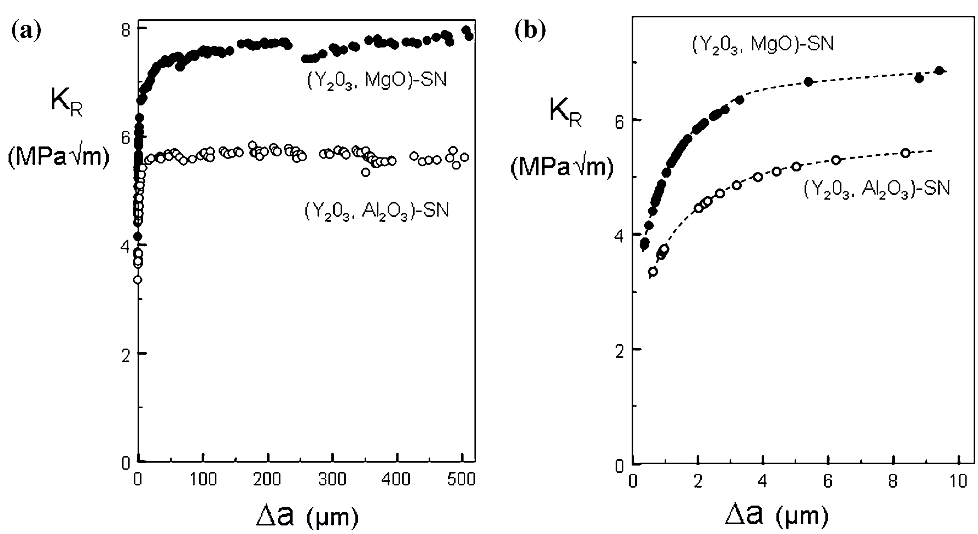

Fig. 1 **a** R-curves for two Si_3N_4-ceramics, **b** initial parts of the R-curves in more detail

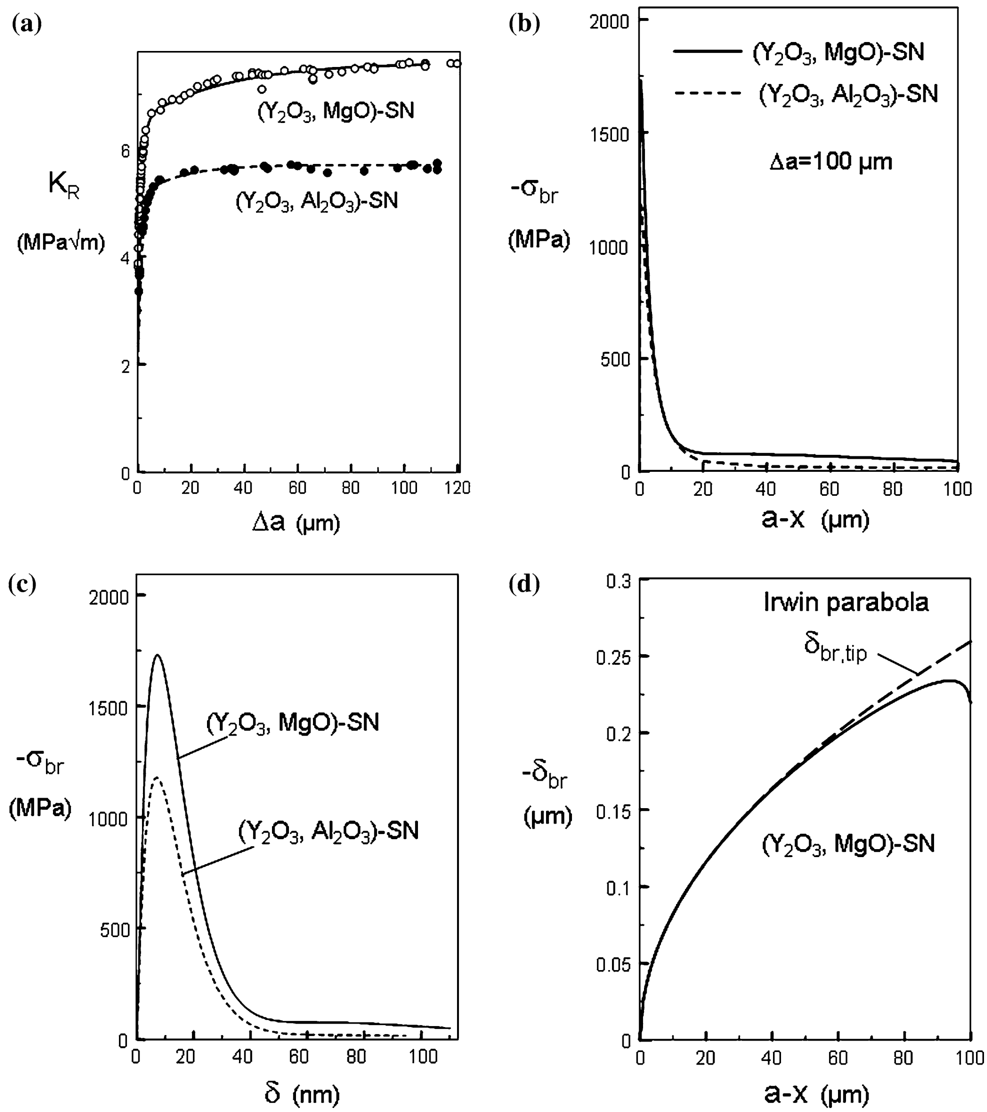

Fig. 2 **a** K_R fitted by Eq. 7 for the two Si_3N_4 ceramics as curves (symbols: results from Fig. 2), **b** bridging stress distribution over the length of a crack with $\Delta a = 100$ μm, **c** bridging stresses versus crack opening displacement, $\sigma_{br} = f(\delta)$, **d** bridging stress displacements for the (Y_2O_3, MgO)-containing Si_3N_4 determined from Eq. 4 (solid curve) and Irwin parabola according to (6) for the same bridging stress intensity factor (dashed curve) for $\Delta a = 100$ μm

The iterative solution establishes the inner loop of a computer program. In the outer loop, the actual crack length is varied and for any chosen crack increment, $\Delta a = a - a_0$, the bridging stress intensity factor, K_{br}, is computed via Eq. 3 and the crack resistance ,K_R, by Eq. 1. If this is done for a number of N crack length values we obtain N computed K_R-values. In a second iterative procedure, the N coefficients A_n are changed systematically (e.g. by application of an optimization procedure [12]) until the computed and the measured K_R are identical. For an acceleration of convergence it is recommended to smooth the measured R-curve and to eliminate experimental scatter.

The results for the two Si_3N_4 ceramics are represented in Fig. 2. Figure 2a shows the measured data (circles) together with the fit-curves. In Fig. 2b, the distribution of the bridging stresses for crack extensions up to $\Delta a = 100$ μm are plotted. For Si_3N_4 with (Y_2O_3, MgO), maximum bridging stresses of $\sigma_{max} = -1730$ MPa are reached at a crack-tip distance of $a - x = 0.4$ μm ($\delta = 7.3$ nm). Silicon nitride with (Y_2O_3, Al_2O_3) shows $\sigma_{max} = -1180$ MPa at $a - x = 0.5$ μm ($\delta = 7$ nm). The bridging relations $\sigma_{br}(\delta)$ are plotted in Fig. 2c. Finally, Fig. 2d shows for (Y_2O_3, MgO) the distribution of the bridging displacements by the solid curve together with the near-tip solution (dashed curve) as resulting from the Irwin relation for $K = K_{br}$:

$$\delta_{br,tip} = \sqrt{\frac{8}{\pi}\frac{K_{br}}{E'}}\sqrt{a - x} \tag{6}$$

It can be seen that there is no strong deviation from the exact result. For a simple approximate evaluation, Eq. 6 can be used instead of Eq. 4.

The fitted R-curves introduced in Fig. 2a by the curves can be expressed as

$$K_R = K_{I0} + C_0[1 - \exp(-C_1\Delta a)] + C_2[1 - \exp(-C_3\Delta a)] \quad (7)$$

with $C_0 = 4.18$ MPa$\sqrt{m}$, $C_1 = 0.8$/µm, $C_2 = 1.09$MPa$\sqrt{m}$, $C_3 = 0.0309$/µm (Δa in µm) for the Si_3N_4 with (Y_2O_3, MgO)-content. The result for the (Y_2O_3, Al_2O_3) containing Si_3N_4 is represented by $C_0 = 3.11$ MPa$\sqrt{m}$, $C_1 = 0.7$/µm, $C_2 = 0.59$ MPa$\sqrt{m}$, $C_3 = 0.06587$/µm.

For $\delta \le 40$ nm, the related bridging laws can be approximated by

$$\sigma_{sh} = \sigma_{br} \approx \sigma_0 \frac{\delta}{\delta_0} \exp[-\delta/\delta_0] \quad (8)$$

with $\sigma_0 = -4670$ MPa, $\delta_0 = 73$ nm for the material with (Y_2O_3, MgO)-content and $\sigma_0 = -3290$ MPa, $\delta_0 = 70$ nm for the silicon nitride with Y_2O_3 and Al_2O_3.

A fit relation over an extended displacement range of $0 \le \delta \le 100$ nm which includes the lower bridging stresses (~ -100 MPa) at displacements $\delta > 40$ nm reads for the (Y_2O_3, MgO)-containing Si_3N_4

$$\sigma_{br} \approx \sigma_0 \frac{\delta}{\delta_0} \exp[-\delta/\delta_0] + \sigma_1 \exp[-\delta/\delta_1] \quad (9)$$

with $\sigma_0 = -4300$ MPa, $\delta_0 = 70$ nm, $\sigma_1 = -150$ MPa, $\delta_1 = 90$ nm.

As an application of the bridging stresses we finally computed the R-curve for a semi-circular crack by using the procedure given in [13]. For this purpose Eqs. 1–4 have to be solved with the weight function for the semi-circular crack given by

$$h_{semi-circ} = \frac{2r[1 + c(1 - r/a)]}{\sqrt{\pi a (a^2 - r^2)}}, \quad c = \frac{0.04 + 0.104(1 - \sin\varphi)^2}{1 - \frac{\pi}{4}} \quad (10)$$

(for r see insert in Fig. 3). The result for the two silicon nitrides is illustrated in Fig. 3. The R-curves for the semi-circular cracks are slightly below those obtained from the edge cracks. This is in agreement with the general result of [13].

Discussion

The bridging stresses for small crack opening displacements were found to be very high with maximum values in the order of $-\sigma_{br} = 1200$–1700 MPa. As a general result from theory, it should be emphasised that the crack extension Δa in which the R-curve shows the high steepness must correspond to the distance from the crack tip in which these stresses act.

Of course, our result cannot be generalized to be a result for all silicon nitride materials. The high bridging stresses will only hold for Si_3N_4 with strongly rising R-curves. In this context, it should be mentioned that many data are available in literature which show a rather moderately rising crack resistance with nearly doubling K_R after crack propagation in the order of about 0.5–2 mm (see e.g. [14, 15]). Such curves must trivially result in moderate bridging stresses.

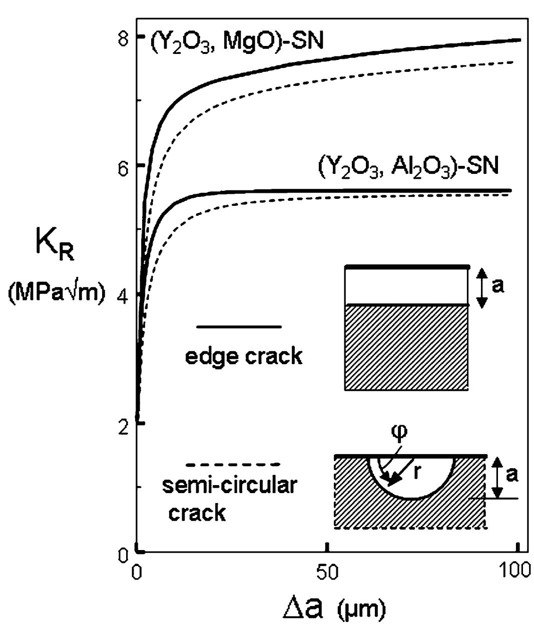

Fig. 3 R-curves for semi-circular cracks (*dashed curves*) computed from the bridging stresses obtained from edge cracks according to the procedure in [13]

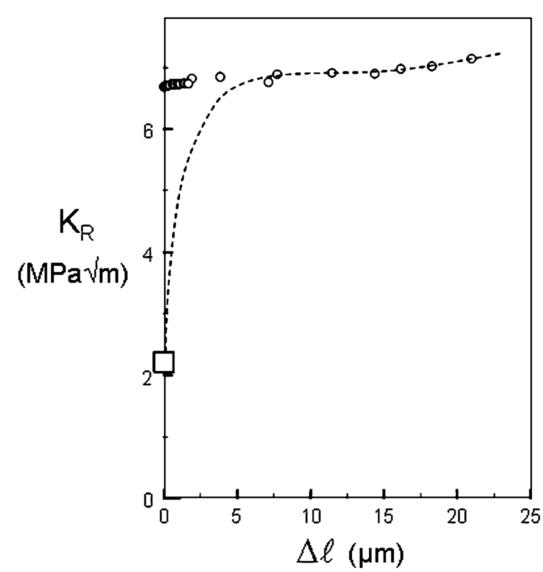

Fig. 4 Data points of the initial R-curve (*open circles*) computed under the assumption that the notch/crack configuration would act as a crack of total length $a_0 + \Delta a$ (a_0 = length of the initial notch) [9]; dashed curve: result from Fig. 2a, square indicates K_{I0}

The steepness of R-curves predominantly reflects the difference between the low value of the starting value K_{I0} which so far was found to be roughly 2 ± 0.5 MPa$\sqrt{m}$ and the high K_R-values present even after a few µm of crack extension.

For illustration of this fact, let us ignore the existence of the true fracture mechanics problem of a crack in front of a notch. In order to show the consequences, we assume the notch/crack configuration to be a simple long crack that would allow the application of the "long-crack solution" for the stress intensity factor and compliance computation. The originally measured data [9] for the material with (Y_2O_3, MgO)-content evaluated with the "long-crack solution" are illustrated in Fig. 4 by the circles. Based on these data and the K_{I0} (indicated by the square) a nearly step-shaped increase within a crack extension of a fraction of a µm would have to be stated. Consequently, the bridging stresses would result in multiples of the bridging stresses determined in the preceding analysis. The correction due to the notch/crack configuration reduces these stresses clearly.

References

1. Marshall DB, Swain MV (1988) J Am Ceram Soc 71:399
2. Ogawa T, Llorca J (1994) J Am Ceram Soc 77:961
3. Okada A, Hirosaki N (1990) J Mater Sci 25:1656
4. Pezzotti G, Muraki N, Maeda N, Satou K, Nishida T (1999) J Am Ceram Soc 82:1249
5. Pezzotti G, Ichimaru H, Ferroni L (2001) JACS 84(8):1785
6. Kruzic JJ, Cannon RM, Ager JW III, Ritchie RO (2005) Acta Mater 53:2595
7. Fett T, Munz D, Kounga Njiwa AB, Rödel J, Quinn GD (2005) J Eur Ceram Soc 25:29
8. Fett T, Munz D, Thun G, Bahr HA (1995) J Am Ceram Soc 78:949
9. Fett T, Fünfschilling S, Hoffmann MJ, Oberacker R, Jelitto H, Schneider GA (2008) J Am Ceram Soc 91:3638
10. Fünfschilling S, Fett T, Hoffmann MJ, Oberacker R, Jelitto H, Schneider GA (2009) J Mater Sci Lett 44:335
11. Fett T, Munz D (2006) Arch Appl Mech 76:667
12. Harwell Program Library, Subroutine V02AD, AERE Harwell, Didcot, Oxon, OX11 0RA, UK
13. Fett T, Fünfschilling S, Hoffmann MJ, Oberacker R (2008) Int J Fract 153:153
14. Li CW, Yamanis J (1989) Ceram Eng Sci Proc 10:632
15. Nishida T, Hanaki Y (1995) J Am Ceram Soc 78:3113